JAAS

ROYAL SOCIETY OF CHEMISTRY

PAPER

View Article Online
View Journal | View Issue

Cite this: *J. Anal. At. Spectrom.*, 2025, **40**, 2582

Received 5th May 2025
Accepted 4th August 2025

DOI: 10.1039/d5ja00182j

rsc.li/jaas

Development of a SEC-ICP-MS platform for multielement metallobiomolecule profiling and quantitation using a blood serum reference material

Georgia Panagou, [a] Nikos Lydakis-Simantiris [b] and Spiros A. Pergantis *[a]

The characterization of metallobiomolecules in biological fluids is essential for understanding metal homeostasis, biomarker discovery, as well as toxicity assessment. In this work, we present a size-exclusion chromatography inductively coupled plasma mass spectrometry (SEC-ICP-MS) platform for the comprehensive profiling of metallobiomolecules in human serum. This method enables the simultaneous detection and quantitation of ten metals and metalloids (Co, Mg, Ca, Cu, Zn, Fe, Mn, Pb, Se, Hg) within a single sample. The integration of post-column flow injection allows for element calibration, using ionic standards containing EDTA, total element determination following the injection of an acid-diluted blood serum sample, and instrument sensitivity monitoring and correction. Method validation was performed using the certified total element concentration in a human reference material (Seronorm Trace Elements Level 2). Element recoveries exceeded 80% for most analytes, both following total element determination and column elution, confirming the robustness and accuracy of the approach. An on-column EDTA injection strategy effectively mitigated metal/metalloid interactions with the stationary phase, enhancing column recoveries of Co and Zn while preventing cross-contamination

[a]*Environmental Chemical Processes Laboratory, Department of Chemistry, University of Crete, Voutes Campus, Heraklion 70013, Greece. E-mail: spergantis@uoc.gr*

[b]*Analytical and Environmental Chemistry Laboratory, School of Mineral Resources Engineering, Technical University of Crete, Chania 73100, Greece*

Georgia Panagou

Georgia Panagou holds a BSc in Chemistry (2019) and a MSc in Analytical and Environmental Chemistry (2021) from the University of Crete, Greece. Her postgraduate studies were supported by the Onassis Foundation. She is currently a PhD candidate in the Department of Chemistry, University of Crete, supported by a fellowship from the Hellenic Foundation for Research and Innovation. Her research focuses on the development of advanced mass spectrometric methods for elemental speciation analysis in biological systems, with particular emphasis on metalloproteomics. She has also collaborated with the Hellenic Centre for Marine Research on interdisciplinary projects involving the trace element analysis of environmental samples. Her research interests include the development of sensitive analytical methods to support efforts towards a better understanding of the roles of metals and metalloids in biological and environmental systems.

Nikos Lydakis-Simantiris

Nikos Lydakis-Simantiris holds a BSc in Chemistry from the University of Athens, and a MSc and a PhD in Chemistry from the University of Crete. He was a postdoctoral fellow in the Department of Biology at the University of Michigan, USA. He worked as a director of the Laboratory of Analytical Chemistry and of the Laboratory of Soil Science and Plant Diagnostics at the Mediterranean Agronomic Institute of Chania (1999–2002). In 2002, he was appointed as a lecturer of Chemistry at the Technological Educational Institute of Crete. In 2019 he joined as a Professor the Department of Agriculture at the Hellenic Mediterranean University. Currently, he is a Professor in the Department of Mineral Resources Engineering, at the Technical University of Crete. His research interests include the interactions of metals with biological systems at the molecular level and the bioremediation of polluted sites.

between samples. This platform expands the number of elements that can be simultaneously monitored and quantified, and maximizes the information obtained for the analysis of each sample, providing an improved assessment of metal/metalloid distributions in human blood serum. The analysis of Seronorm Trace Elements Level 2 material provided novel insights into the element distribution across different relative molecular mass metallobiomolecules. Detected metallobiomolecule bands aligned with biomolecules known to be present in human serum and previous studies of this reference material, yet discrepancies in element distribution suggest possible element addition during reference material preparation. Its ability to provide detailed elemental distributions across biomolecular bands enhances its potential for applications in biomarker discovery, disease monitoring, and environmental exposure assessments.

1. Introduction

Metallobiomolecules, a diverse group of biomolecules that include metals or metalloids, are essential to numerous biological processes.[1] It is estimated that at least one-third of all known proteins require a metal ion for their proper function.[2] These molecules, including metalloproteins, metallopeptides, and metal-binding cofactors, play indispensable roles in enzymatic catalysis, structural stabilization, electron transport, and signal transduction.[3] Essential metals, such as magnesium (Mg), calcium (Ca), iron (Fe), zinc (Zn), copper (Cu), manganese (Mn), cobalt (Co), nickel (Ni), molybdenum (Mo), and selenium (Se) are integral to these processes.[4] For instance, Fe enables oxygen transport in hemoglobin,[5] Zn supports enzymatic activity and immune function,[6] and Se provides antioxidant defense through selenoproteins.[7] However, the balance of these metal–biomolecule interactions is crucial, as dysregulation can lead to pathological states. In contrast to essential metals, toxic metals and metalloids such as arsenic (As), cadmium (Cd), and lead (Pb) disrupt biological systems, often interfering with essential metal pathways and inducing oxidative stress or carcinogenesis. For example, As exposure is linked to cancer and cardiovascular diseases,[8] Pb impairs neural development,[9] and Cd adversely affects kidney function and bone health.[10] Consequently, studying metallobiomolecules is critical for understanding the role of essential and toxic metals in biological systems and their implications for health and disease.[11]

Analyzing metallobiomolecules presents significant analytical challenges.[12] A key difficulty lies in preserving the native metal–protein interactions throughout all the analytical steps, since these interactions are often non-covalent and influenced by factors such as pH and ionic strength.[13] This may lead to metal ions dissociating from their corresponding metallobiomolecules, as well as their replacement by other metal ions present in the sample, *e.g.* during sample preparation.[14] Furthermore, the absence of well-characterized metallobiomolecule standards further complicates quantitative and qualitative analyses.[15]

A variety of analytical methods are used for the detection, and quantitation of metallobiomolecules or/and the characterization of metal–protein interactions.[16] Hyphenated techniques, such as liquid chromatography (size-exclusion, anion-exchange, reversed-phase) coupled with inductively coupled plasma mass spectrometry (ICP-MS),[17] or atomic emission spectrometry (ICP-AES),[18] enable the separation and sensitive detection of metalloproteins by their metal content. Similarly, capillary electrophoresis (CE) coupled with ICP-MS is also used, for metalloprotein analysis, due to the high-resolution separation it offers, but with several other limitations.[19] Gel electrophoresis, including native and denaturing approaches, like SDS-PAGE, is employed to separate proteins based on size or charge, often followed by metal-specific staining or detection using laser ablation ICP-MS.[20,21] MS techniques, such as MALDI-MS and ESI-MS, as well as tandem MS techniques and top-down proteomics approaches are useful for identifying metalloproteins, providing information about their structure, and characterizing metal–protein interactions and metal binding sites.[22,23] Other methods like immobilized metal affinity chromatography (IMAC) target proteins with metal-binding properties,[24] while non-destructive techniques such as X-ray absorption spectroscopy (XAS) provide insights into the oxidation state and

Spiros A. Pergantis

Spiros A. Pergantis has a BSc in Chemistry from the University of Ioannina, Greece, and a PhD in Chemistry from the University of British of Columbia, Canada. He has worked as a National Research Council Postdoctoral Fellow with the US Environmental Protection Agency. His first academic position was a lectureship in Analytical Chemistry at Birkbeck College, University of London. In 2003, he joined the Department of Chemistry, University of Crete, Greece, where he is currently a Professor of Analytical Chemistry. His research interests include the development of advanced molecular and atomic mass spectrometric methods for elemental speciation analysis (As, Se, Sb, Cr) in environmental and biological systems. This includes the detection and characterization of unknown compounds, especially those found in environmental matrices. His research in atomic mass spectrometry has led to advancements in single particle and single cell ICP-MS for the determination of metal-containing nanoparticles (Ag, Au), as well as the metal content of individual biological cells, respectively. Some of the approaches he has developed are based on ion mobility separations, hydrodynamic liquid chromatography, and chip-based microfluidics, and their hyphenation to ICP-MS.

coordination environment of metals.[25] In addition, chemoproteomic techniques utilize functionalized probes that covalently bind biomolecules interacting with metals, allowing for enhanced separation, identification, and imaging of metal–protein interactions.[26] Computational tools for metal-binding site prediction further complement experimental approaches.[27]

Size-exclusion chromatography (SEC) coupled with ICP-MS has emerged as a powerful analytical approach for studying metallobiomolecules. SEC is a gentle separation technique where molecules are separated based on their hydrodynamic size, in the absence of direct interaction with the stationary phase, whilst preserving the native state of biomolecules, and therefore metal–protein interactions.[28] SEC is considered a robust technique that enables the direct analysis of biological samples with complex matrices.[17] When coupled with ICP-MS, it allows for sensitive and multi-elemental analysis, enabling the determination of relative molecular mass distributions and associated metal content in a single run.[29,30] SEC-ICP-MS, while valuable for metallobiomolecule analysis, has limitations. Low salt concentrations required for compatibility with the mass spectrometers can cause nonspecific protein or/and metal-column interactions. Its relatively poor resolution limits use to biomolecule fractionation or screening, and reliance on elution volumes and external standards puts limitations on accurate molar mass matching or definitive protein identification.[1,14]

The SEC-ICP-MS method counts numerous applications for metallobiomolecule analysis in blood plasma[28,31,32] and serum,[33–36] as well as in other biological samples, such as cerebrospinal fluid,[37] tissue extracts,[17,38] and cell cultures.[39,40] However, the majority of the studies utilizing SEC-ICP-MS focus on a limited number of elements per analysis (typically 1 to 5), leaving essential and toxic elements underexplored. These restrictions underscore the need for methodological advancements to enhance the capabilities of SEC-ICP-MS, maximizing the information gained from single sample analysis and expanding its applications in metallobiomolecule research.

The sample of interest in this study is blood serum, as it is a potentially informative and convenient sample for metallobiomolecule profiling. It serves as a dynamic interface between the external environment and internal organs, and thus can potentially provide critical insights into health status, exposure to environmental toxins, and metal homeostasis.[16,41] Moreover, blood serum offers advantages from the analytical methodology aspect as it does not require pretreatment.

Therefore, the objective of the present study was the development of an SEC-ICP-MS platform that enables, in a single analytical run: (1) the simultaneous detection of metallobiomolecules containing one or more of 13 elements (Co, Mg, Ca, Cu, Zn, Fe, Mn, Pb, Se, Hg, S, P, and I), (2) the quantitation of elements in each detected metallobiomolecule band, and (3) the determination of total element concentrations in blood serum samples, along with instrument stability monitoring, aiming to advance the field of metallomics (metalloproteomics) by addressing current analytical challenges. Moreover, the proposed platform was used for the multielement metallobiomolecule analysis of Seronorm™ Trace Elements Serum Level 2 (Seronorm-L2), a human blood serum reference material well-established for its total metal/metalloid concentrations. However, to our knowledge, studies on its metallobiomolecule profile remain limited.[35,42] Understanding the metal distribution within biomolecules in this reference material is essential for its effective use in method validation, quality control, and interlaboratory comparisons, particularly in metalloproteomics and clinical research.

2. Methods and materials

2.1 Reagents, chemicals, and reference material

Ammonium acetate (CH_3COONH_4, ≥98%), ethylenediaminetetraacetic acid (EDTA, ≥99%), nitric acid (HNO_3, ≥69%), *t*-octylphenoxypolyethoxyethanol (Triton X-100), thyroglobulin from bovine thyroid (670 kDa, ≥90%), apo-transferrin (77.8 kDa, ≥98%), bovine serum albumin (monomer 66.4 kDa, dimer 132.8 kDa, ≥96%), beta-casein from bovine milk (24.0 kDa, ≥98%), α-lactalbumin from bovine milk (14.2 kDa, ≥85%), cytochrome-c from equine heart (12.4 kDa, ≥98%), methylcobalamin (1344 Da, ≥97%), and Met-Arg-Phe-Ala acetate salt (524 Da, ≥90%) were obtained from Sigma-Aldrich (Massachusetts, USA).

Single-element standards for Co, Ca, Mg, Cu, Zn, Fe, Mn, Se, Hg, Pb, As, Ni, Cd, and Cr of 10 000 mg L^{-1} in 4% HNO_3 were purchased from CPI International (California, USA). Seronorm™ Trace Element Level 2 blood serum reference material was purchased from SERO AS (Hvalstad, Norway). For the preparation of all solutions, ultrapure water of 18.2 MΩ cm^{-1} was used (PURELAB Option-S, Elga Labwater, UK).

2.2 Instrumentation and operating parameters

The chromatography system used consisted of a LC-AD-20 pump (SHIMADZU, Kyoto, Japan) delivering mobile phase (100 mM CH_3COONH_4, pH 7.2) to the size exclusion column Discovery® BIO GFC 150 (30 cm × 4.6 mm, SUPELCO, Seelze, Germany), at a flow rate of 0.7 mL min^{-1}. The system includes a switching valve (EV700-100, Rheodyne, California, USA) positioned before the size-exclusion column (SEC) and a manual sample injector (Model 7010, Rheodyne, California, USA) located immediately after. Both injectors are equipped with a 100 μL loop. The post column injector is coupled with a peristaltic pump (Spetec GmbH, Erding, Germany), for loop loading, and with a NexION 350X inductively coupled plasma mass spectrometer (ICP-MS) equipped with Syngistix software (PerkinElmer, Massachusetts, USA). The ICP-MS was operated in kinetic energy discrimination mode by supplying the collision cell with 2 mL min^{-1} He. Each acquisition was carried out in time-resolved analysis mode, for 34 isotopes and for a total of 35 min per analytical run. All SEC-ICP-MS instrumental parameters are listed in Table S.1.

2.3 Standard solutions and samples preparation

2.3.1 Blood serum preparation for total metal concentration determination. Seronorm-L2 was reconstituted by adding

3 mL of ultrapure water to the lyophilized human blood serum material, according to the manufacturer's instructions.

For total metal concentration determination, a 0.05% Triton X-100 solution in 0.5% HNO_3 (Triton X-100 solution) and an 8 mM EDTA solution in 100 mM CH_3COONH_4 (pH 7.2, EDTA solution) were prepared. A volume of 100 μL Seronorm-L2 was diluted with 900 μL of 0.05% Triton X-100, and after 30 min the sample was further diluted with the appropriate volume of mobile phase and EDTA solution, so the total dilution factor was 20 and the final EDTA concentration was 80 μM. Samples were stored in an ice bath until analysis.

2.3.2 Standard solutions. Elements were divided into four groups, based on the typical element concentration in human blood serum, under normal conditions.[43,44] The higher abundance metals: Mg, Ca, Zn, Cu, and Fe, (group 1) the medium abundance elements: Se (group 2) and Co, Ni, Mn (group 3), and low abundance elements: Hg, Pb, As, Cd, and Cr (group 4). For each group, a standard stock solution was prepared by using single-element standard solutions. These were combined and further diluted in the mobile phase. An appropriate volume of EDTA solution was added to all standard solutions, to achieve a final concentration of 80 μM EDTA. The final element concentrations in the standard solutions were 50, 250, and 500 μg L^{-1} for group 1 elements; 4, 20, and 40 μg L^{-1} for Se; 1, 5, and 10 μg L^{-1} for group 3, and 0.5, 2.5, and 5 μg L^{-1} for group 4. An additional multielement standard solution containing all elements was made, and used as a sensitivity control during the analysis. This control contains 50 μg L^{-1} of elements in group 1; 0.5 μg L^{-1} of group 2; 3 μg L^{-1} Se, and 1 μg L^{-1} of group 4 elements.

2.4 Detailed injection protocol for sample analysis

The proposed SEC-ICP-MS approach includes 4 injections performed at specific intervals. An initial on-column injection of the blood serum sample is made at the beginning (0 s) of the analysis. Two post-column injections of the sample and the sensitivity control standard are conducted before the chromatography dead time (400 s). More specifically, the diluted blood serum is injected at 200 s, for total element concentration determination, and the sensitivity control standard is injected at 300 s, for instrumental stability monitoring. Biomolecule elution takes place within the 460–1200 s time window. Finally, on-column injection of the 8 mM EDTA solution is made at 550 s, and the metal–EDTA complexes formed in the column are eluted, after the end of the chromatographic analysis (1400–1600 s) (Fig. 1). The injection protocol and observed elution times are also listed in detail in Table S.2.

2.5 Quantitation method validation

Quantitation of total element concentrations in diluted blood serum and element concentration corresponding to each detected chromatographic peak is performed using an external calibration curve. The calibration curve is generated through post-column injection of a series of multielement standard solutions at the start of each experimental day. The calibration procedure for total element concentration determination was validated in terms of linearity, sensitivity, precision, and accuracy.

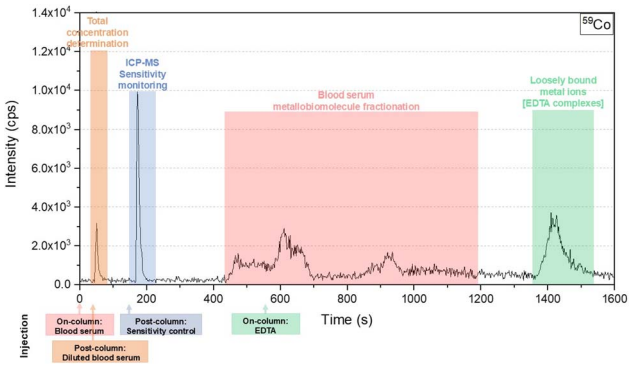

Fig. 1 SEC-ICP-MS chromatogram for ^{59}Co obtained from the analysis of Seronorm-L2, using the developed approach. The on-column or post-column injection time of blood serum (red), 8 mM EDTA (green), diluted blood serum sample (brown), and sensitivity control (blue) are indicated with an arrow below the *x*-axis. Peaks are assigned to the corresponding solution and indicated using their corresponding colour.

2.5.1 Linearity and range. The linearity and dynamic range of the quantitation method were validated to ensure accurate quantitation of metals in blood serum samples. Linearity was assessed using standards containing elements at concentrations expected in typical blood serum samples, ensuring the method's applicability to real-world analyses. To further validate the method's robustness, linearity was also evaluated across a broader concentration range from 1 to 500 μg L^{-1} for all elements under study (except Hg and Cr). Post-column injection peaks from standard solutions were integrated using OriginPro 2018 (OriginLab, Massachusetts, USA), and calibration curves were generated based on peak areas. The correlation coefficient (R^2) was used to assess the linearity between element concentration and signal response.

2.5.2 Limit of detection and limit of quantitation. To ensure that the analytical method is capable of detecting and accurately quantifying each element at the specified levels, the limits of detection (LOD) and limits of quantitation (LOQ) were determined from the respective calibration curve data, made after triplicate analysis of each multielement standard. To calculate the LOD and LOQ, the residual standard deviation (S_y) and the slope (s) of each regression line were used (eqn (1) and (2), respectively).[45]

$$\mathrm{LOD} = 3.0 \times \frac{S_y}{s} \quad (1)$$

$$\mathrm{LOQ} = 10 \times \frac{S_y}{s} \quad (2)$$

2.5.3 Quantitation correction. Instrumental sensitivity drift is one of the two main contributors to the measurement uncertainty of elements by ICP-MS.[46] As the probability of instrumental drift increases with the time of analysis, and the sample analysis is 35 minutes, it was important to take sensitivity drift into consideration.

To account for potential instrumental sensitivity drifts between samples, a multielement calibration standard solution (sensitivity control) was injected post-column, as a part of each sample analysis. If the intensity difference between the latest and the initial calibration standard measurement, for a given element, exceeded 20%, the latest measurement was used to perform a new single-point calibration. In this case, the element concentration was calculated directly by relating the measured chromatographic peak area ($\text{Area}_{\text{element}}$) of the element to the peak area ($\text{Area}_{\text{S.C.}}$) and known concentration ($C_{\text{S.C.}}$) of the sensitivity control standard (eqn (3)).

$$C_{\text{element}} = \text{Area}_{\text{element}} \times \frac{C_{\text{S.C.}}}{\text{Area}_{\text{S.C.}}} \quad (3)$$

2.5.4 Accuracy and precision. Reference material Seronorm-L2 was analyzed in triplicate to assess the accuracy and precision of the analytical method.

The post-column flow injection peak obtained for diluted Seronorm-L2 (Fig. 1, diluted blood serum), for each element, was integrated, and the total element concentration was determined using an external calibration curve. The recovery of each element and the standard deviation of the three replicates were calculated (eqn (4)).

$$\text{Recovery}\% = \frac{\text{measured total concentration of element}}{\text{certified total element concentration}} \times 100\% \quad (4)$$

Seronorm-L2 is not certified for the presence of individual metallobiomolecules, therefore column recovery was calculated in two ways. The sum of element concentration across all detected chromatographic peaks (400–1200 s) was compared to (a) the certified (indicative) concentration value provided for Seronorm-L2 and (b) the total element as determined by the pc-FI of the diluted blood serum (eqn (5)).

$$\text{Column recovery}\% = \frac{\text{sum of element concentration in all detected chromatographic peaks}}{\text{(a) certified/indicative or (b) determined total element concentration}} \times 100\% \quad (5)$$

3. Results and discussion

3.1 Development of a multielement metallobiomolecule speciation platform

As the objective of this study was to size-fractionate and quantitate the metallobiomolecules present in blood serum, an advanced SEC-ICP-MS speciation platform was developed. First of all, the SEC component allowed for the size fractionation of each element, revealing each element's distribution amongst biomolecules of different sizes, with multielement detection being conducted using on-line ICP-MS. Chromatographic recoveries were also determined for each element by using the platform's post-column flow injection (pc-FI) component. This allowed for total metal concentration determination by analyzing an additional volume of the serum sample in pc-FI mode within the chromatography's dead time (Fig. 2). To monitor for instrument drift a multielement standard was also injected in the dead time in the pc-FI mode for each sample analyzed. Injecting within the chromatographic dead time prevents overlapping with chromatographically eluting metallobiomolecules. Finally, an EDTA solution was injected on-column at a retention time that did not allow for it to affect the elution of the sample metallobiomolecues, but provided column flushing of retained metal ions. Overall, the metallobiomolecule speciation platform developed here allows for metal-containing biomolecule size fractionation, quantitation of total metal/metalloid, quantitation of each metal/metalloid size band, determining column recoveries and improving them, and finally being able to achieve improved mass balances for each metal/metalloid.

3.1.1 Metallobiomolecule size fractionation and multielement detection by on-line SEC-ICP-MS. The Discovery® BIO GFC 150 column, with a fractionation range of 0.5 to 150 kDa, was used to screen a broad range of metallobiomolecule sizes. Ammonium acetate was selected as the mobile phase for its compatibility with both ICP-MS and ESI-MS, enabling metal detection and providing further potential for biomolecule identification in a single chromatographic setup, providing the basis for a comprehensive approach to metallobiomolecule determinations.

The separation of metallobiomolecules by SEC was evaluated by using a protein mixture containing thyroglobulin (670 kDa), bovine serum albumin (monomer 66.4 kDa, dimer 132.8 kDa), beta-casein (24.0 kDa), cytochrome-c (12.4 kDa), methylcobalamin (1.3 kDa) and Met-Arg-Phe-Ala acetate salt (0.5 kDa). Separation efficiency and time of analysis were monitored as a function of flow rate, which was increased from 0.5 to 1 mL min^{-1}, with 50 mM or 100 mM of CH_3COONH_4 as the mobile phase. Proteins were detected by their S content using ICP-MS with a dynamic reaction cell (DRC), containing O_2 gas, while thyroglobulin and cytochrome-c, were also observed by their I and Fe content, respectively (Table S.3).[32] Methylcobalamine was detected by its P and Co content. The best separation efficiency in the lowest time of analysis was achieved with 100 mM of CH_3COONH_4 as the mobile phase, at a flow rate of 0.7 mL min^{-1}. The applied chromatography operation parameters are listed in Table S.1. The SEC column was calibrated using the same protein mixture, with the addition of apotransferrin and α-lactalbumin (bovine milk) to provide additional reference points for more precise size calibration and performance monitoring (Fig. S.1). Both of these added proteins were also detected by their S content.

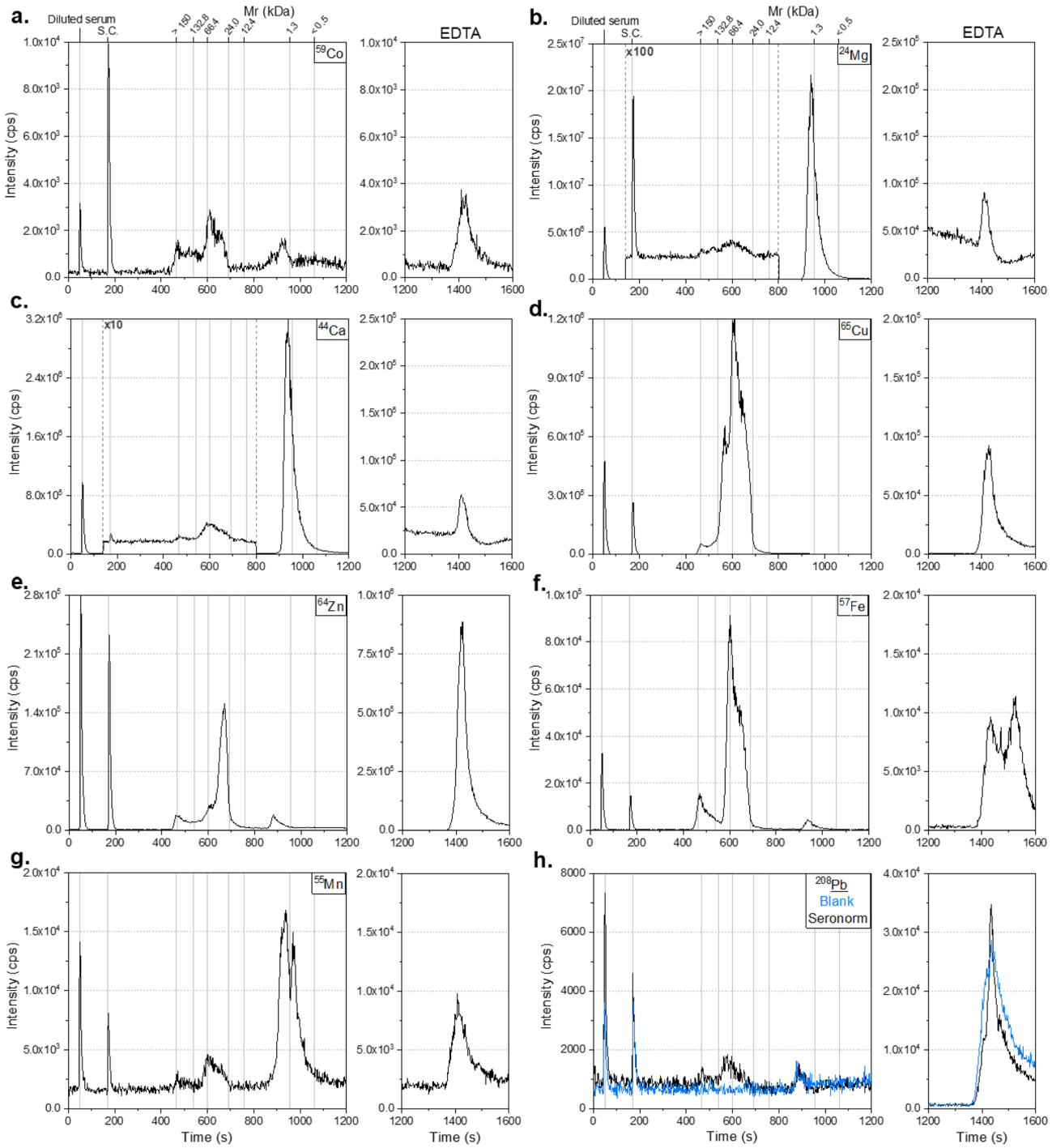

Fig. 2 Metal–biomolecule profiles of Seronorm-L2 obtained by using the proposed SEC-ICP-MS method. Post-column injections of diluted Seronorm-L2 (50 s) and sensitivity control standard (S.C., 180 s), metal–biomolecule chromatogram (450–1200 s) and metal–EDTA complex elution after the 8 mM EDTA on-column injection (1300–1600 s) for cobalt (a), magnesium (b), calcium (c), copper (d), zinc (e), iron (f), manganese (g), and lead (h). Data in the Mg (b) and Ca (c) chromatogram sections indicated by vertical dashed lines (150–800 s) were magnified by a factor for clarity purposes. (h) Blue graph: post-column injection of dilution process blank [0.025% Triton-X, 0.25% HNO_3, 80 μM EDTA, 100 mM CH_3COONH_4 (50 s), S.C. (180 s), Pb–biomolecule chromatogram of mobile phase on-column injection] (450–1200 s), and Pb–EDTA complex elution (1300–1600 s).

While DRC mode was applied for monitoring protein standards during method development, for metallobiomolecule detection *via* the presence of a metal, metalloid, or other heteroatom in serum samples Kinetic Energy Discrimination (KED) mode with He gas was used. KED mode offers significant advantages as it reduces polyatomic interferences while allowing for the monitoring of metallobiomolecules by their S content.[47] Monitoring S provides complementary insights into

the composition of metallobiomolecule bands and supports the identification of sulfur-rich biomolecules, such as metallothioneins.

The He gas flow rate was optimized during the analysis of a blood serum sample with online SEC-ICP-MS in the range from 2.0 to 3.0 mL min^{-1}. The use of blood serum is expected to efficiently assess matrix effects and the behavior of the metallobiomolecules under KED mode, ensuring optimal detection of metal/metalloids without compromising sensitivity. The He flow rate increase from 2 to 2.5 mL min^{-1} caused a significant reduction in the intensities of all elements, without a corresponding proportional background reduction. Further KED gas flow rate increase, led to lower background levels for Fe, Ca, Mg, Mn, S, and P, but caused a 2 to 3 times intensity reduction, compared to 2.0 mL min^{-1}, which counteracted the background reduction benefits. As a result, 2.0 mL min^{-1} was chosen as the optimal He gas flow rate for this type of multielemental speciation analysis, providing reduced polyatomic interferences and a better signal-to-noise ratio for all elements under study, compared to standard mode analysis.

3.1.2 Detection and quantitation of low relative molecular mass ionic species. Despite the suitability of SEC for the fractionation of metallobiomolecules in complex matrices, there is a concern regarding secondary interactions that may occur between the metal ionic species and the stationary phase. Such interactions can affect the elution time of metal species or even cause their adsorption to the stationary phase.[29]

To study the presence of secondary interactions in the SEC column and their effects on the element ionic species elution time, a multielement standard solution containing 10 μg L^{-1} of each metal or metalloid in the form of Co^{2+}, Mg^{2+}, Ni^{2+}, Cu^{2+}, Zn^{2+}, Mn^{2+}, Pb^{2+}, Ca^{2+}, Fe^{3+}, Cd^{2+}, Cr^{6+}, $HAsO_4^{2-}$, and SeO_4^{2-} in 100 mM CH_3COONH_4 was injected on-column. From the obtained chromatograms it was observed that none of the injected ionic metal/metalloid species were eluted within the expected time based on their relative molecular mass (M_r), approximately 1060 s, confirming the presence of secondary interactions, which impact the chromatographic procedure. Inorganic species of Mg, Ca, As, Hg, and Cr eluted between 870–900 s, whereas Se and Mn eluted slightly later at 900–920 s and 950–1050 s, respectively (Fig. S.2 and S.3). Small amounts of Co (0.5 μg L^{-1}) and Cu (1.3 μg L^{-1}) were also detected at 870–890 s, suggesting that, in addition to secondary interactions that may shift elution earlier, significant adsorption to the stationary phase occurs. The effect was even stronger for Zn, Ni, Pb, and Fe, as they were not detected within the main elution window (400–1200 s) or in the extended range (1200–1600 s), even at higher injection concentrations (20–50 μg L^{-1}; Fig. S.4).

The observed premature elution of small ions suggests that these species may inefficiently access the stationary phase pores, potentially due to electrostatic repulsion between the charges they may carry and exposed silanol groups on the stationary phase or metal ions and other cationic species already retained on the column as part of the stationary phase-mobile phase equilibrium. Differences in elution times and adsorption levels indicate that the impact of secondary interactions varies depending on the specific ion, likely due to differences in charge, coordination chemistry, and affinity towards the stationary phase.

To recover the metal ions that do not elute from the column, a high-concentration EDTA solution was injected. Specifically, an 8 mM EDTA solution in 100 mM CH_3COONH_4 was introduced after analyzing the 10 μg L^{-1} standard of ionic species, leading to the elution of Co, Cu, Zn, Ni, Pb, and Fe as metal–EDTA complexes. The concentration of eluted Co matched the estimated total adsorbed amount (9.7 μg L^{-1}). However, accurate quantitation of Cu, Zn, Ni, Pb, and Fe in the metal–EDTA band was challenging due to high background signals in the blank, introducing significant uncertainty. A higher concentration of 10 mM EDTA was also tested, but it did not result in improved metal recoveries.

While secondary interactions affect the detection and quantitation of Zn, Ni, Pb, and Fe free ions, they are less concerning in blood serum analysis, where these elements are not expected in their free ionic form. Nonetheless, monitoring metal–EDTA complex bands remains a useful approach, particularly when the free ionic fraction in a sample is high. These findings highlight the importance of accounting for secondary interactions when interpreting results and implement measures that maximize column recoveries while preventing cross-contamination during analysis.

The EDTA injection time was optimized to avoid interaction with eluting metallobiomolecules and to minimize overall analysis time. Since EDTA–metal complex detection begins approximately 800 s after injection, a 550 s delay between sample and EDTA injections was sufficient to prevent overlap with the metallobiomolecule elution window. Accordingly, EDTA was injected at 550 s, allowing full elution of EDTA–metal complexes within a total run time of 35 minutes. Subsequent samples were injected immediately after.

3.1.3 Multielement quantitation by post-column calibration. The quantitation of metallobiomolecules by using ionic standards faces several difficulties, as metal ions may be retained on the column as already discussed. Moreover, the use of metallobiomolecule standards is not applicable for many elements, due to their limited commercial availability. To enable the determination of element concentration in blood serum, as well as in all detected metallobiomolecule bands, by using multielement ionic standards, a post-column flow injection (pc-FI) procedure was utilized. By using pc-FI, direct interaction of metal ions with the SEC stationary phase and therefore loss of analytes is avoided.

For the calibration procedure optimization, multielement ionic standards containing 1 to 500 μg L^{-1} of all elements under study, in 100 mM CH_3COONH_4, were analyzed by consecutive pc-FI. Linear regression of the resulting areas as a function of element concentration revealed a poor linearity for Ca, Zn, Cu, Pb, and Cd, due to metal loss during the analysis. To address this issue, EDTA was added to the standard solutions to chelate the metal ions and therefore minimize their interaction with the introduction system. Two EDTA concentrations were tested across all standards in triplicate: 80 μM, as it is comparable to the total metal ion concentration of the highest concentration standard (105.3 μM), and 160 μM EDTA, to provide an excess of

Table 1 Correlation coefficient R^2 for 1–500 μg L^{-1} range and calibration range. Limit of detection (LOD) and limit of quantitation (LOQ) values of elements under study as calculated from their corresponding calibration curves obtained by post-column standards injection procedure

Element	Concentration range (μg L^{-1})	R^2 value	R^2 value (1–500 μg L^{-1})	LOD (μg L^{-1})	LOQ (μg L^{-1})
Co	0–10	0.9999	0.9993	0.13	0.43
Mg	0–1000	0.9999	1.0000	17.05	56.82
Ca	0–1000	0.9992	0.9998	60.93	203.10
Cu	0–1000	0.9999	0.9996	15.33	51.10
Zn	0–500	0.9999	1.0000	6.54	21.80
Fe	0–500	0.9998	1.0000	22.11	73.71
Mn	0–10	0.9996	0.9990	0.43	1.42
Pb	0–5	0.9984	0.9995	0.33	1.11
Se	0–40	0.9995	1.0000	1.56	5.21
Hg	0–5	0.9995	—	0.19	0.62
As	0–5	0.9994	0.9996	0.20	0.68
Ni	0–10	0.9991	1.0000	0.49	1.64
Cd	0–5	0.9898	1.0000	0.05	0.17
Cr	0–5	0.9993	—	0.31	1.02

EDTA relative to the metal ions in the multielement standards. The presence of EDTA (80 μM) enhanced linearity and recovery for all metal ions across the 1–500 μg L^{-1} concentration range (Table 1). Increasing EDTA concentration to 160 μM showed no additional benefits, so 80 μM EDTA in all multielement standards was chosen as the optimal condition for post-column flow injection calibration.

3.1.4 Total element determination procedure. For total element concentration determination in blood samples by ICP-MS, acid decomposition and direct sample dilution with various reagents are the most widely used methods for sample preparation.[48] In the proposed approach, the direct sample dilution method was employed for total element concentration determination by pc-FI, as it is simple, rapid, effective, and has a minimal risk of metal and metalloid contamination.[49] Specifically, a ten-fold dilution in a non-ionic surfactant Triton X-100 (0.05%) and diluted HNO_3 (0.5%) (referred to as Triton-X100 solution) was selected to reduce possible matrix effects by increasing protein and lipid membrane solubilization and reducing the sample's viscosity.[50,51]

As Triton X-100 may affect the signal intensity of elements, due to its carbon content, and the nebulization efficiency as a surfactant,[52] a further dilution of the sample in 100 mM CH_3COONH_4 was included. To optimize the second dilution factor, Seronorm-L2 diluted in Triton X-100 solution was further diluted two, five, and ten-fold and was analyzed by using pc-FI. To avoid any metal loss during the analysis, 80 μM EDTA was also added to the diluted samples. Comparison of recoveries across these conditions revealed that the ten-fold dilution resulted in lower recoveries for all elements. For the two-fold and five-fold dilutions, recoveries of all elements differed by less than 10% from the certified or indicative values, indicating minimal effect of dilution factor within this range. Given the negligible difference between the two- and five-fold dilutions, the two-fold dilution was selected to ensure that trace elements concentration in real blood serum samples will not be below LODs. Following this optimization a ten-fold dilution of blood serum samples with the Triton X-100, followed by a two-fold dilution with 100 mM CH_3COONH_4 and 80 μM EDTA was chosen as the dilution method for the total element determination.

3.2 Multielement quantitation method validation and Seronorm-L2 analysis

3.2.1 Correlation coefficients, LOD and LOQ. Multielement standards were made, as described in Section 2.3, to include the expected element concentration ranges in human blood serum. The regression equation and correlation coefficient values (R^2) were calculated using linear regression analysis. For all elements the R^2 values were greater than 0.9984, indicating satisfactory linearity not only within the concentration range used for Seronorm-L2 analysis but also within 1 to 500 μg L^{-1} of multielement ionic standards, confirming the method's capability to accurately determine metal concentrations both within and beyond the expected physiological levels (Table 1). The method's sensitivity was determined by calculating the LOD and LOQ of all the elements (Table 1). The low LOQ ensures that even trace amounts of the metal can be accurately quantified, making the method highly suitable for monitoring the low-level concentrations of some elements present in blood serum samples.

3.2.2 Recovery assessment and metallobiomolecule profiling of Seronorm-L2. To further evaluate the performance of the SEC-ICP-MS platform, total and column recovery studies were conducted using a certified human serum reference material, providing insights into the accuracy and precision of quantitation across all target elements (Table S.4).

Given the need for well-characterized reference materials in metallobiomolecule analysis, Seronorm-L2 was selected for quantitation method validation and to explore its metallobiomolecule profile using the developed SEC-ICP-MS platform. Previous studies have examined Se speciation (selenoproteins and selenoamino acids)[35] and monitored its Fe, Zn, Cu, and Se speciation differences with Seronorm Trace Elements Serum Level 1 by strong anion exchange

chromatography.[42] However, to our knowledge, its multielement metallobiomolecule profile has not been systematically studied by using SEC. In the following sections we describe the chromatographic behavior of each element, and provide the concentrations of their elution bands in Table 2. The assigned relative molecular mass ranges are approximate, as the elution time of metallobiomolecules depends on their hydrodynamic size and can be affected by secondary interactions with the stationary phase.

3.2.2.1 Cobalt. The total Co concentration in Seronorm-L2 reference material was determined to be 2.6 ± 0.2 μg L^{-1} using the pc-FI capability of the SEC-ICP-MS method. The resulting $^{59}Co^{+}$ peak can be seen in Fig. 2a at approximately 50–60 s. Based on the Seronorm-L2 certified value (2.7 μg L^{-1}), the recovery of total Co concentration was determined to be 94.9% ± 9.8%.

The second peak at approximately 180–200 s corresponds to a 0.5 μg L^{-1} Co-containing multielement standard also injected in pc-FI. When signal intensity did not change by more than 20% no corrections were made for instrument drift.

Column recovery, another key parameter determined using this method, was calculated from the sum of Co concentrations corresponding to all the chromatographic peaks detected from 400–1200 s (2.3 ± 0.2 μg L^{-1}) and comparing them to the total Co determined as described previously. Thus, column recovery for Co was determined to be 88.7% ± 12.7%. When the reference material's certified Co concentration was used, column recovery was determined to be 83.4% ± 7.2%. These slightly lower recoveries indicate strong adsorption of small amounts of Co onto the SEC column. This occurrence was confirmed when injecting an 8 mM EDTA solution at 550 s gave an expected Co–EDTA peak at approximately 1400 s. The inclusion of this Co–EDTA peak in the column recovery calculations gave an enhanced recovery of 104.6% ± 3.4% (2.7 ± 0.3 μg L^{-1}).

In the Co–biomolecule elution profile section of the SEC-ICP-MS chromatogram (400–1200 s), Co was mainly detected in biomolecule bands with a M_r greater than 24 kDa. This finding is consistent with previous studies on human serum, where the majority (94.3%) of Co was associated with high M_r biomolecules (>50 kDa).[53] Specifically, four partially resolved Co-containing bands were observed in the range from 24 kDa to the upper exclusion limit of 150 kDa, with the highest concentration peak corresponding to the 24–66 kDa band, likely resulting from the elution of albumin, which is a major Co carrier in the blood.[54,55] The second band in this range may be attributed to transcobalamin II (43 kDa), a B12-vitamin transporter.[56] Another band in the 66.4–132.8 kDa range could correspond to haptocorrin (~120 kDa), which binds approximately 80% of B12-vitamin in serum. The band observed above 132.8 kDa may include albumin dimers[55,57] and other B12-dependent enzymes, such as methionine synthase (~140 kDa).[58] These enzymes are present in whole blood, but they can be released into the serum due to cell lysis during the preparation of the reference material. Additionally, a significant amount of Co was detected in two bands within the 1.3–12.4 kDa range, which may include free vitamin B12. This is likely the result of its dissociation from the aforementioned

Table 2 Element concentration detected in each chromatographic band, and as M–EDTA complex ([M-elementl) from the analysis of Seronorm-L2. Total element concentration eluted from the column ([eluted total]). The assigned relative molecular mass (M_r) of each band is based on the approximate M_r range corresponding to the peak apex and the majority of each peak's elution profile

	Range of relative molecular masses										
	From		132.8	66.4	24.0	12.3	1.3	0.5			
Element	To	>150	150	132.8	66.4	24.0	12.3	1.3	<0.5	[M–EDTA]	[Eluted total]
Co (μg L^{-1})		0.17 ± 0.05	0.32 ± 0.08	0.51 ± 0.04	0.40 ± 0.02	n.d.	(1) 0.13 ± 0.01 (2) 0.30 ± 0.01	0.41 ± 0.09[a]	n.d.	0.43 ± 0.46	2.68 ± 0.34
Mg (μg L^{-1})		5.19 ± 2.53	11.26 ± 1.7	52.7 ± 5.9	5.5 ± 3.4		31.2 ± 1.0 mg L^{-1}[a]	n.d.	n.d.	27.8 ± 6.8	31.2 ± 1.0 mg L^{-1}
Ca (mg L^{-1})		0.16 ± 0.04	1.50 ± 0.09			n.d.	91.2 ± 3.4[a]	n.d.	n.d.	0.95 ± 0.06	93.8 ± 3.6
Cu (μg L^{-1})		35.6 ± 4.0	422.98 ± 23.82	1.47 ± 0.78 mg L^{-1}		n.d.	11.8 ± 2.5	8.1 ± 1.0	n.d.	81.4 ± 7.1	2.03 ± 0.11 mg L^{-1}
Zn (μg L^{-1})		19.7 ± 2.4	16.86 ± 1.21	185.4 ± 6.7		n.d.	15.8 ± 2.1	5.47 ± 0.27[a]	n.d.	891 ± 53	1134 ± 63
Fe (μg L^{-1})		279 ± 18		1965 ± 120		n.d.	45.0 ± 1.6	14.9 ± 5.0	n.d.	n.d.	2304 ± 143
Mn (μg L^{-1})		0.28 ± 0.06	0.26 ± 0.05	1.54 ± 0.15		n.d.	5.9 ± 0.1	4.2 ± 0.1[a]	n.d.	n.d.	12.1 ± 0.1
Pb (μg L^{-1})		0.14 ± 0.01	n.d.	0.49 ± 0.02	n.d.	n.d.	0.04 ± 0.01	n.d.	n.d.	n.d.	0.68 ± 0.04
Se (μg L^{-1})		28.4 ± 2.7	6.6 ± 2.6		(1) 13.2 ± 1.9 (2) 12.7 ± 1.2	n.d.	n.d.	57.3 ± 1.5[a]	n.d.	n.d.	118.2 ± 4.3
Hg (μg L^{-1})		0.58 ± 0.02	0.61 ± 0.07		0.6 ± 0.1	n.d.	n.d.	n.d.	n.d.	n.d.	1.79 ± 0.17

[a] Ionic species are included. n.d.: not detected.

transporter proteins, as free vitamin B12 is not typically present in significant amounts in blood.[59]

3.2.2.2 Magnesium. The total Mg concentration determined by pc-FI of the diluted Seronorm-L2 was 36.0 ± 1.4 mg L^{-1}, in line with the certified value (35.7 mg L^{-1}), giving a recovery of 100.8% ± 3.9%. The concentration of Mg eluted from the column was 31.2 ± 1.0 mg L^{-1}, corresponding to a column recovery of 86.9% ± 1.1% relative to the determined total, and 87.5% ± 2.8% using the certified value. The injection of 8 mM EDTA resulted in an insignificant (~0.1%) recovery.

In the Mg–biomolecule profile of the SEC-ICP-MS chromatogram (400–1200 s; Fig. 2b), the majority of Mg was detected in the form of low M_r species (900–1200 s). In this elution time, low M_r neutral species and Mg ions are co-eluting, as shown from the analysis of 10 μg L^{-1} Mg^{2+} standard solution (Fig. S.2). Smaller amounts of Mg were associated with higher M_r biomolecules in three bands, one around 66.4 kDa and two bands within the 134.8 to 150 kDa range. These findings are in agreement with the literature, which reports that most Mg in human blood serum exists in its free ionic form (~65%) and is complexed with small anions (~15%), such as phosphates, and a smaller portion (~20%) is bound to proteins.[60] Protein-bound Mg is mainly found in albumin (~70%), and smaller amounts are found interacting with globulins.[61,62]

3.2.2.3 Calcium. By pc-FI, the total Ca concentration was determined to be 92.8 ± 3.5 mg L^{-1}, giving a total recovery of 82.4% ± 5.2% relative to the certified value (138 mg L^{-1}). The Ca concentration eluted from the column was 75.9 ± 2.9 mg L^{-1}, which corresponds to a column recovery of 81.8% ± 3.1% based on the determined total, and 67.3% ± 2.5% relative to the certified value. EDTA injection resulted in a slight increase (~1%) in recovery.

In the Ca-biomolecule profile of the SEC-ICP-MS chromatogram (400–1200 s; Fig. 2c), the majority of Ca was detected as low M_r species (900–1200 s), consistent with its well-documented presence as a free ion in blood serum. Co-elution studies using a 10 μg L^{-1} Ca^{2+} standard solution (Section 3.1.1) confirm that these low M_r species primarily consist of free Ca^{2+} ions and/or small Ca-containing complexes. Additionally, lower amounts of Ca were also associated with higher M_r biomolecules in two or possibly three bands: two in the 66.4 and 22.4 (minor) kDa range, and a third one in the higher than 150 kDa range. These findings align with literature reports indicating that the majority of Ca in blood serum exists in its free ionic form, with 10% of it being complexed with small anions, such as phosphates and bicarbonates. While smaller amounts of Ca are bound to albumin and globulins, such as immunoglobulin G.[63,64] These proteins may be included in the 24.0–66.4 kDa band and >150 kDa band observed in the Ca–biomolecule profile, respectively.

The amount of Ca detected in high-M_r biomolecules (2%) was significantly lower than what is expected for serum samples (40%). While the exact cause of this discrepancy remains unclear, several factors could contribute to this observation. Potential explanations include differences in the formulation of the reference material, such as variations in total protein concentration, or the presence of stabilizing agents that may alter Ca binding to proteins. Also, it has been suggested that the concentrations of Cu, Fe, and Se in Seronorm-L2 may result from the external addition of these elements in their ionic forms.[35,42] If ionic Ca was also added during preparation, this could explain the higher proportion of non-bound Ca^{2+} detected. However, further investigation would be needed to determine the exact cause of the observed shift in Ca-bound ratios.

3.2.2.4 Copper. The total Cu concentration determined *via* pc-FI was 1.83 ± 0.03 mg L^{-1}, corresponding to 84.0% ± 1.5% recovery relative to the certified Seronorm-L2 value (2.18 mg L^{-1}). The concentration of Cu eluted was 1.95 ± 0.11 mg L^{-1}, giving a column recovery of 106.6% ± 3.9% when compared to the determined total, and 89.7% ± 5.0% relative to the certified value. The post-elution injection of the EDTA solution did not affect Cu recovery.

SEC-ICP-MS chromatographic profiling (400–1200 s; Fig. 2d) revealed the presence of four main Cu-containing bands in Seronorm-L2. Specifically, one band was detected to be associated with biomolecules with M_r higher than 150 kDa, one band within the 132.8–150 kDa range, and two bands between the 24.0–66.4 kDa range. Lower amounts of Cu were detected to be present with lower M_r species (<12.4 kDa).

The high-M_r band at 460–520 s may include transcuprein (~270 kDa), which binds 7–15% of serum Cu,[65] and smaller amounts of extracellular Cu/Zn-SOD3 (135 kDa).[66] The band within 66.4–132.8 kDa can be attributed to ceruloplasmin (~132 kDa), the primary Cu transporter in the blood (~60% of total serum Cu).[36,67] The peak retention times at approx. 620 s and 660 s (24.0–66.4 kDa) may correspond to Cu-bound albumin (10–15% of serum Cu) and intracellular Cu/Zn-SOD1 (32 kDa), respectively.[68] Cu/Zn-SOD1 is mainly present intracellularly, but low levels can be found in the serum due to cell lysis.[69] Low Cu concentration (<0.5%) was detected in the <12.3 kDa range, possibly as Cu–amino acid complexes.[70,71] The overall Cu distribution is consistent with prior serum speciation studies.[68,72]

However, its distribution pattern amongst biomolecules is altered, as the Cu concentration associated with biomolecules with M_r lower than 66.4 kDa is higher than the measured band that is attributed to ceruloplasmin. Such an alteration could be reasonable in the case of Cu ion addition during the reference material preparation, shifting Cu binding dynamics among serum biomolecules. The external addition of Cu ions could lead to non-specific binding with other serum components that, under physiological conditions, participate in the exchangeable Cu^{2+} regulation in the blood, such as albumin.[71] This is supported by the notably higher total Cu concentration in Seronorm-L2 (2.18 mg L^{-1}) compared to typical serum Cu levels in healthy individuals (620–1070 μg L^{-1}) or patients with certain pathological conditions, such as cancer (up to ~1700 μg L^{-1}).[68,72]

3.2.2.5 Zinc. The total Zn concentration determined *via* pc-FI was 1.27 ± 0.04 mg L^{-1}, corresponding to 60.7% ± 1.7% recovery relative to the certified value (2.09 mg L^{-1}). The eluted Zn concentration was 0.24 ± 0.01 mg L^{-1}, resulting in a column recovery of 19.2% ± 0.4% based on the determined total, and 11.6% ± 0.6% relative to the certified value. The on-column

injection of EDTA solution released 1.14 ± 0.06 mg L^{-1} of retained Zn, improving column recovery to 89.4% ± 3.5% and 54.3% ± 3.0%, respectively. These results indicate that a substantial portion of Zn was retained by the column and subsequently eluted with EDTA, suggesting significant secondary interactions between Zn species and the stationary phase. Such interactions have also been reported for Zn on anion exchange columns, often resulting in poor reproducibility and elevated background signals.[42] However, in the proposed SEC-ICP-MS method, the on-column injection of 8 mM EDTA not only improved recovery but also maintained reproducible results and stable background levels, even after seven consecutive serum analyses (data not shown).

The SEC-ICP-MS profile (400–1200 s, Fig. 2e) revealed Zn associated with five M_r bands: one above 150 kDa (450–500 s), one around 132.8 kDa (500–560 s), two within 24.0–132.8 kDa (560–750 s), and one in the 1.3–12.4 kDa range (850–950 s). The high-M_r band at 450–500 s likely corresponds to α2-macroglobulin (~720 kDa), a protease inhibitor that strongly binds Zn in blood.[73] The 132.8 kDa band is consistent with SOD3, which incorporates both Cu and Zn as cofactors (4 Cu and 4 Zn atoms).[66] The main Zn transporter in serum is albumin, which can be present in the 24.0–66.4 kDa range.[74,75] The second peak detected in that range aligns with Cu/Zn-SOD1 (~32 kDa), and other Zn-binding proteins such as haptoglobin (38.7 kDa) and the heavy chain of immunoglobulins (42.4 kDa).[76] The low-M_r band likely corresponds to Zn-containing metallopeptides, including metallothioneins, as reported in previous serum studies.[77]

The observed Zn distribution in the Zn–biomolecule chromatographic profile deviates from previously reported patterns in human blood serum, where Zn is primarily bound to albumin (~80%), with smaller bands associated with α2-macroglobulin (~10–20%).[78] However, Zn exhibits weak interaction with albumin, making it the greater part of the loosely bound or exchangeable Zn pool in circulation. As a result, a significant portion of albumin-bound Zn may have dissociated from the protein during the chromatographic separation, becoming retained by the column's stationary phase and subsequently being eluted as a Zn–EDTA complex. Zn–biomolecule analysis could be improved by employing an alternative SEC column or by changing the mobile phase composition in order to minimize interactions between labile Zn-complexes and the stationary phase, and thus prevent or minimize their dissociation. However, when optimizing for Zn, when performing multielement speciation analysis, the affinity of the stationary phase for the other elements must also be considered in order to maintain good overall method performance. Some examples of Zn–biomolecule complex profiles using alternative SEC columns have been published.[79,80]

3.2.2.6 Iron. The total Fe concentration determined *via* pc-FI was 2.08 ± 0.16 mg L^{-1}, corresponding to a recovery of 100.8% ± 7.7% based on the certified value (2.07 mg L^{-1}). The amount of Fe eluted from the column between 400 and 1200 s was 2.30 ± 0.13 mg L^{-1}, yielding a column recovery of 108.0% ± 4.5% relative to the determined total, and 111.3% ± 3.9% relative to the certified value. No significant Fe elution was observed after EDTA injection, relative to the blank, indicating negligible retention of Fe on the column.

The obtained Fe–biomolecule chromatographic profile revealed the presence of Fe in multiple M_r ranges, specifically a wide band within the 132.8–150 kDa range, two in the 24.0–132.8 kDa, and one in the 1.3–12.3 kDa (400–1200 s, Fig. 2f). The majority of Fe was detected in the 24.0–132.8 kDa, in the band corresponding to biomolecules of M_r around 66.4 kDa (peak height max ~600 s), which likely includes transferrin (~75 kDa), the primary Fe-transport protein in blood serum.[81] The second band observed within the same range, with a lower Fe concentration, is likely associated with non-transferrin proteins such as albumin (66.4 kDa) and hemoglobin (64.5 kDa), which are found at lower concentrations in blood serum, under physiological conditions.[82] In the M_r range above 132.8 kDa, Fe detection in the band (450–560 s) suggests its association with serum ferritin (~480 kDa), the main iron-storage protein.[83] Small amounts of Fe were also detected in the 1.3 kDa range, likely corresponding to Fe complexes with citrate ions, which represent a minor band of total serum Fe.[82]

3.2.2.7 Manganese. With pc-FI, the total Mn concentration in Seronorm-L2 was determined to be 15.0 ± 1.3 μg L^{-1}, corresponding to a recovery of 105.5% ± 9.5% compared to the Mn certified value (14.2 μg L^{-1}). A total of 12.1 ± 0.1 μg L^{-1} Mn was eluted from the column, between 400–1200 s, resulting in a column recovery of 81.5% ± 7.4% relative to the determined value and 85.5% ± 0.8% relative to the certified concentration. Compared to the blank, no additional Mn amounts were detected as a result of the post-elution EDTA injection.

In Mn–biomolecule profile (400–1200 s; Fig. 2g) six Mn-associated bands were observed. Two bands were detected in the higher than 132.8 kDa range, likely corresponding to Mn-containing enzymes, such as α2-macroglobulin (450–490 s) and oxalate oxidase (~140 kDa) (490–550 s).[37,84] A significant amount of Mn was also detected in the 24.0–66.4 kDa range (550–700 s), where two partially overlapping bands are observed. This elution time fits well with the presence of transferrin (~78 kDa)[85] and albumin (~66 kDa), which are the main Mn transport proteins in blood serum.[37,86,87] The majority of Mn was detected in the low-M_r range, with two primary bands eluting within the 0.5–12.4 kDa range (peak height max ~920 s and ~980 s, respectively). Previous studies on blood serum Mn speciation have suggested that low-M_r Mn species correspond to Mn complexes with citrate (up to ~700 Da) and amino acids.[88,89] The lowest M_r Mn band eluted at a similar time as the ionic Mn standard, indicating the presence of ionic Mn and/or small Mn complexes. Mn species around ~1.3 kDa likely result from interactions between free Mn ions or Mn–citrate complexes and small peptides, as Mn binds peptides containing metal-coordinating residues.[90] However, further investigation is needed to confirm the presence of such interactions in blood serum.

The Mn distribution observed in Seronorm-L2 differs significantly from previous reports on Mn speciation in human serum, where ~88% of the total 1.7 ± 0.8 μg L^{-1} Mn detected (as compared to the 14.2 μg L^{-1} in Seronorm-L2) was associated with transferrin and albumin, followed by Mn-enzymes (~10%),

with only 2% present in low-M_r species.[37] These discrepancies could indicate the intentional or unintentional addition of Mn or other metal ions to the reference material, which may lead to the formation of the previously mentioned Mn complexes or the displacement of Mn ions from their native biomolecule carriers.

3.2.2.8 Lead. Pb in the 20-fold diluted Seronorm-L2 sample was below the LOD (0.33 μg L^{-1}), as expected from the Seronorm-L2 indicative concentration (1.29 μg L^{-1}). To evaluate method performance, the diluted sample was spiked with 10 μg L^{-1} Pb, giving a total 11.29 μg L^{-1} Pb. This spike concentration level aligns with the range of total serum Pb concentrations reported for healthy individuals (up to 60 μg L^{-1}) and well below levels observed in certain medical conditions (up to 220 μg L^{-1}).[91,92] Triplicate analysis of the spiked diluted sample yielded a mean of 10.2 ± 0.1 μg L^{-1}, corresponding to a recovery of 90.5% ± 1.2%.

Total Pb recovery during the chromatographic SEC-ICP-MS analysis of the non-diluted, non-spiked, Seronorm-L2 (400–1200 s; 0.68 ± 0.04 μg L^{-1}) gave column recoveries of 52.5% ± 3.2%, relative to the Seronorm-L2 indicative Pb concentration value. This indicates that a significant amount of Pb remained adsorbed to the stationary phase, however, the injection of EDTA did not result in additional Pb being eluted compared to the blanks (Fig. 2h), possibly due to either the stronger interaction of Pb with the stationary phase compared to EDTA, or the inability to determine such a low concentration of Pb present in the Pb–EDTA peak (approximately 0.61 μg L^{-1}). Pb recovery, similarly to that of Zn, could be improved by using a SEC column with lower affinity towards Pb ions, although all method changes should also take into account the all other elements being analysed.

The SEC-ICP-MS chromatographic profile (400–1200 s; Fig. 2h) showed that Pb was primarily associated with biomolecules within the 24.0–132.8 kDa range. Pb in blood is predominantly protein-bound, with up to 40% complexed with albumin, while the remaining is associated with thiol-containing ligands.[93] Study of Pb-binding proteins reveals a significant hemoglobin binding capacity, which could also be present, alongside albumin, in the detected band (530–650 s).[94] Thus this analysis confirms the binding of Pb to large serum proteins, such as hemoglobin and/or albumin.

3.2.2.9 Selenium. The total Se concentration in Seronorm-L2, determined *via* pc-FI, was 128.3 ± 6.5 μg L^{-1}, corresponding to 92.3% ± 4.7% recovery relative to the certified value (139 μg L^{-1}, 111–167 μg L^{-1}). The concentration of Se eluted from the column (400–1200 s; Fig. 3a) was 118.2 ± 4.3 μg L^{-1}, resulting in a column recovery of 92.3% ± 5.3% and 85.0% ± 3.1% compared to the pc-FI determined and the certified concentration, respectively. The injection of 8 mM EDTA did not affect Se recovery, as the inorganic oxo-Se species present in the sample do not form stable complexes with EDTA.

In the Se–biomolecule profile chromatogram, Se was detected in five bands. The presence of multiple Se-containing biomolecules in human serum has been well-documented, with Se primarily incorporated into Selenoprotein P (SelP, ~61 kDa),[95] glutathione peroxidase (GPx, ~92 kDa),[96] and albumin (SeAlb), with progressively lower associated concentrations.[97–99] Additionally, a separate study has reported the presence of other Se-containing proteins, such as an isoform of SelP (47 kDa) and a 41.1 kDa Se-containing protein.[100]

Based on the literature, the Se band detected in the 66.4–132.8 kDa can be attributed to GPx, and the two bands in the 24.0–66.4 kDa to SeAlb and SelP. The Se concentration for each band is listed in Table 3. A previous study on Se speciation in Seronorm-L2, using two-dimensional affinity chromatography coupled with ICP-MS, identified SelP, GPx, and SeAlb with the last two having similar concentrations, as shown in Table 3.[35] Additionally, this study reported a high concentration of inorganic Se (iSe), suggesting that the total Se concentration in this reference material was achieved through the external addition

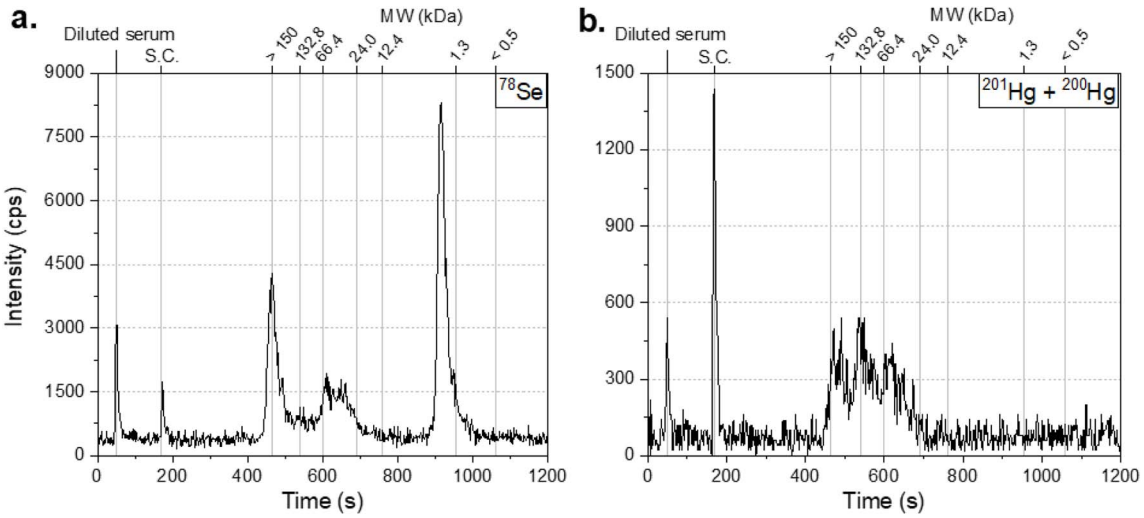

Fig. 3 Metal–biomolecule profiles of Seronorm-L2 obtained by the proposed SEC-ICP-MS method. Post-column injections of diluted Seronorm-L2 (50 s) and sensitivity control standard (S.C., 180 s), and metal–biomolecule chromatogram (450–1200 s) for selenium (a) and mercury (b). The Hg–biomolecule chromatogram depicts the sum of ^{201}Hg and ^{200}Hg intensities for clarity purposes.

Table 3 Se concentrations in Se-containing albumin (SeAlb), glutathione peroxidase (GPx), selenoprotein P (SelP), and inorganic Se species (iSe) of Seronorm L-2, analyzed using the proposed SEC-ICP-MS platform (present study) and double affinity column coupled to ICP-MS (Jitaru *et al.*, 2010).[35] The M_r range corresponding to the elution time of each Se-species in SEC-ICP-MS and the respective fraction eluted in dcAF-ICP-MS are also provided

Method	SEC-ICP-MS (present study)		dcAF-ICP-MS[a] (Jitaru *et al.*)[35]
Species	M_r band range (elution time)	Se concentration (μg L^{-1})	Fraction
High M_r (SelP)	>150	28.4 ± 2.7	—	—
GPx	66.4–132.8	6.6 ± 2.6	—	Void volume
SeAlb	24.0–66.4 (580–620 s)	13.2 ± 1.9	16 ± 1	Blue-sepharose
SelP	24.0–66.4 (620–700 s)	12.7 ± 1.2	47 ± 1	Heparin-sepharose
iSe	1.3–12.4	57.3 ± 1.5	—	Void volume
GPx + iSe		63.9 ± 4.1[b]	72 ± 1	
SelP + high M_r		41.1 ± 3.9[b]	47 ± 1	

[a] Double affinity columns: Hitrap Heparin-Sepharose and Hitrap Blue-Sepharose. [b] Calculated values for comparison purposes.

of iSe to blood serum. The Se detected in the band at 900–1000 s aligns with the elution time of a selenate standard solution (Fig. S.2), and its concentration aligns with the previously proposed inorganic Se addition.

While these two studies show agreement in the speciation and Se concentrations of GPx, SeAlb, and iSe, a notable discrepancy is observed in the Se concentration associated with the SelP band. Jitaru *et al.*[35] reported that 47 ± 1 μg L^{-1} of Se, identified as SelP, eluted from a Heparin-Sepharose (HS) column, however, in the present study, the Se concentration associated with the M_r of SelP is significantly lower (12.7 ± 1.2 μg L^{-1}).

Moreover, significant Se levels were also detected at 450–500 s corresponding to M_r of higher than 150 kDa. Previous analyses of human serum and heparin-isolated SelP fraction analyzed by SEC-ICP-MS, have also reported the elution of SelP before GPx or albumin despite its lower M_r.[101,102] The reason for this discrepancy is not explicitly addressed, however, it is plausible that SelP multiple cysteine and selenocysteine residues allow it to form disulfide or selenodisulfide bridges with other proteins, which could result in higher M_r complexes.[95,103] Additionally, deviations from the expected elution time may occur in SEC, as separation is based on hydrodynamic size rather than exact M_r. To confirm the heparin affinity of the Se-containing biomolecule detected at 460–500 s, selenoproteins in Seronorm-L2 were fractionated using a HiTrap Heparin-Sepharose column (7 mm (i.d.) × 25 mm, GE Healthcare, Uppsala, Sweden). For this purpose, 250 μL of Seronorm-L2 was injected into the column using 50 mM CH_3COONH_4 (pH 7) as a binding buffer. After 5 min, bound proteins were eluted using 1.5 M CH_3COONH_4 (pH 7), as the elution buffer, for 5 min. Fractions of 0.5 mL were collected in microtubes for the span of 5 min. The flow rate of binding and elution buffer was 1 mL min^{-1}. Se levels of each fraction were monitored by FI analysis and 100 μL of the fraction with the highest Se concentration was injected into the SEC-ICP-MS system. The Se-containing biomolecule was again detected at 460–500 s, confirming its affinity with heparin.

The presence of two peaks corresponding to SelP may be explained by the two main isoforms found in human plasma (61 kDa and 51 kDa).[103,104] The 51 kDa isoform includes significantly lower Se content, which could reduce its ability to cross-link with other proteins and contribute to the observed M_r differences. However, further investigation is needed. The combined Se concentration eluted at 460–500 s and 620–700 s (41.1 ± 3.9 μg L^{-1}) closely matches the Se concentration in the heparin-bound fraction (SelP) reported by Jitaru *et al.*,[35] further supporting this interpretation.

3.2.2.10 Mercury. The total Hg concentration of Seronorm-L2 was determined to be 2.19 ± 0.46 μg L^{-1}, *via* pc-FI, aligning well with the indicative value of 2.27 μg L^{-1} and yielding a recovery of 96.6% ± 20.6%. Hg detected in chromatographic peaks was 1.79 ± 0.17 μg L^{-1} (400–1200 s; Fig. 3b), giving a column recovery of 84.8% ± 24.0% relative to the measured value, and 78.8% ± 7.4% when compared to the indicative concentration.

In SEC-ICP-MS chromatographic profiling, three distinct Hg-associated bands were detected. Due to the high affinity of Hg species with thiol- and seleno-groups, it can be found primarily in S-rich and Se-containing biomolecules.[105] The 132.8 kDa band and the 24–66.4 kDa band are likely associated with the selenoproteins GPx, and SelP, respectively, consistent with previous studies.[106,107] Additionally, in the 66.4 kDa band, albumin may also be included, as it is known to interact with Hg through its thiol-containing residues.[108] The high-M_r band (>150 kDa) could correspond to the Se-containing biomolecule, having the same elution time (attributed to SelP), or other high-M_r molecules with significant S content, such as α2-macroglobulin.[48] The absence of significant low-M_r Hg species indicates that Hg in Seronorm-L2 is predominantly protein-bound, with minimal presence as free ions or small complexes.

3.2.2.11 Arsenic, nickel, cadmium, and chromium. Attempts to quantify total concentrations of As, Ni, Cd, and Cr in Seronorm-L2 using pc-FI revealed several analytical challenges, primarily related to low element concentrations and spectral interferences. The concentrations of all four elements in the 20-fold diluted Seronorm-L2 fell below their respective LOD (0.20 μg L^{-1} As, 0.49 μg L^{-1} Ni, 0.05 μg L^{-1} Cd, and 0.31 μg L^{-1} Cr), making element spiking necessary to assess recovery and method performance. In spiked Seronorm-L2 containing a total

of 10.38 μg L^{-1} As, 29.5 μg L^{-1} Ni, 10.12 μg L^{-1} Cd, and 13.91 μg L^{-1} Cr, concentration recoveries ranged from 111% to 148%. These elevated values indicate a significant signal enhancement, likely due to the formation of polyatomic species caused by the complex blood serum matrix containing multiple elements at high concentrations.

SEC-ICP-MS analysis of undiluted Seronorm-L2, also revealed substantial overestimations in the concentrations of As, Ni, Cd, and Cr (Fig. S.5). For As, elevated column recovery (159% ± 10%) was attributed to polyatomic species, such as $^{43}Ca^{16}O_2^+$ and $^{40}Ca^{35}Cl^+$, formed due to high Ca^{2+} (approx. 138 mg L^{-1} Ca) and Cl^- (3.4–3.7 mg L^{-1} Cl in serum samples under normal conditions)[109] concentrations, which co-eluted with As between 950 and 1010 s (Fig. S.6). Even after excluding this As band, the recovery remained above 100%, indicating residual interferences likely associated with other polyatomic ions like $^{40}Ar^{35}Cl^+$ and $^{36}Ar^{39}K^+$. For Cr, similar issues were encountered, with evidence pointing towards Cl and S-based polyatomic interferences affecting Cr isotopes and leading to overestimated concentrations. Ni concentrations eluting from the column exceeded the certified value (289% ± 12%), which may also be correlated to spectral interferences involving calcium-based ions ($^{44}Ca^{16}O^+$, $^{43}Ca^{16}O^1H^+$).[110] Additionally, the displacement of Ni ions from the stationary phase by serum biomolecules may contribute to higher Ni concentrations detected across multiple elution bands (Fig. S.5b). Cd concentration eluted from the column was an order of magnitude higher than the Seronorm-L2 certified value (0.12 μg L^{-1}). The unaltered $^{114}Cd/^{112}Cd$ ratios for all Cd detected bands (Fig. S.5c) suggest that similarly to Ni^{2+}, Cd^{2+} present in the stationary phase may bind to serum proteins, resulting in co-elution and therefore detection of higher Cd quantities.

Collectively, these findings emphasize the limitations of both pc-FI and SEC-ICP-MS for accurate quantitation of As, Ni, Cd, and Cr in complex biological matrices like serum. Sample preparation strategies to remove high-concentration elements before the analysis and/or method modifications, such as using higher He flow rates in the ICP-MS collision cell, could potentially reduce interferences and improve the analysis of these elements.

4. Conclusions

The proposed SEC-ICP-MS platform enables the efficient metallobiomolecule profiling of nine metals (Co, Mg, Ca, Cu, Zn, Fe, Mn, Pb, and Hg) and one metalloid (Se) in human blood serum. The integration of a post-column flow injection setup enhances the method's capabilities by enabling element quantitation within each metallobiomolecule band using ionic standards. Additionally, the injection of acid-diluted serum samples and a multielement standard during chromatography dead time (0–450 s) allows for total element determination and sensitivity drift monitoring.

The method's wide dynamic range and low LOD and LOQ ensure its applicability to serum samples with both physiological and altered element concentrations, making it a valuable tool for metallobiomolecule studies in pathological conditions and metal toxicity assessments. Analysis of the Seronorm Trace Elements Level 2 reference material confirmed element recoveries exceeding 80% for most metals, demonstrating the method's robustness and accuracy in both total element determination and metallobiomolecule fractionation. The on-column EDTA injection strategy significantly improved column recovery for Co and Zn, effectively eluting metal ions adsorbed onto the stationary phase and preventing cross-contamination between samples. Future work could explore the use of alternative SEC stationary phases with reduced metal ion affinity in order to enhance the recovery of labile metal–biomolecule complexes.

The analysis of Seronorm-L2 by using the SEC-ICP-MS platform provided valuable insights into the M_r distribution of metallobiomolecules and elemental distribution among them. The M_r ranges of detected metallobiomolecules aligned with previous studies of this reference material (Se, Cu, Zn, Fe) and known metallobiomolecules present in human serum (Co, Mg, Ca, Mn, Pb, Hg). However, discrepancies in the element distribution compared to healthy human serum and the detection of significant concentrations of free ionic species support previous speculations of certain elements having been added in their ionic forms (*e.g.*, Se, Fe, Cu, Mn) during reference material preparation.

Overall, in the present study, it was demonstrated that the proposed SEC-ICP-MS platform is a reliable tool for quantitative metallobiomolecule analysis in human serum, offering new opportunities for clinical research, biomarker discovery, and trace element studies in health and disease. The metallobiomolecule profiling of Seronorm-L2 represents a step forward in establishing well-characterized reference materials for metallobiomolecule studies, enhancing the reliability and comparability of future research. Compared to previous SEC-ICP-MS approaches, this platform allows for the simultaneous detection and quantitation of more elements, offering a more comprehensive assessment of metal and metalloid distributions in serum. Its application can be extended to other biofluids, such as blood plasma and urine, as well as other biological samples, with proper sample preparation to ensure compatibility and accuracy.

Author contributions

Georgia Panagou: conceptualization, investigation, methodology, formal analysis, validation, visualization, writing – original draft, and writing – review & editing. Nikos Lydakis-Simantiris: conceptualization, resources, and writing – review & editing. Spiros A. Pergantis: conceptualization, methodology, validation, visualization, resources, funding acquisition, supervision, writing – original draft, and writing – review & editing.

Conflicts of interest

The authors have no conflict of interest to declare.

Data availability

Other relevant data are also available upon request.

The authors confirm that the data supporting the findings of this study are available within the article and its SI. See DOI: https://doi.org/10.1039/d5ja00182j.

Acknowledgements

This research work was supported by the Hellenic Foundation for Research and Innovation (H. F. R. I.) under the 4th Call for HFRI PhD Fellowships (Fellowship Number: 10664).

References

1 S. Mounicou, J. Szpunar and R. Lobinski, *Chem. Soc. Rev.*, 2009, **38**, 1119–1138.
2 V. Putignano, A. Rosato, L. Banci and C. Andreini, *Nucleic Acids Res.*, 2018, **46**, D459–D464.
3 I. H. Ibrahim, *Metalloproteins and Metalloproteomics in Health and Disease*, Elsevier, 2024, vol. 141.
4 M. A. Zoroddu, J. Aaseth, G. Crisponi, S. Medici, M. Peana and V. M. Nurchi, *J. Inorg. Biochem.*, 2019, **195**, 120–129.
5 N. Abbaspour, R. Hurrell and R. Kelishadi, *J. Res. Med. Sci.*, 2014, **19**, 164–174.
6 D. P. Kiouri, E. Tsoupra, M. Peana, S. P. Perlepes, M. E. Stefanidou and C. T. Chasapis, *EXCLI J.*, 2023, **22**, 809–827.
7 V. M. Labunskyy, D. L. Hatfield and V. N. Gladyshev, *Physiol. Rev.*, 2014, **94**, 739–777.
8 K. S. Mohammed Abdul, S. S. Jayasinghe, E. P. S. Chandana, C. Jayasumana and P. M. C. S. De Silva, *Environ. Toxicol. Pharmacol.*, 2015, **40**, 828–846.
9 M. S. Collin, S. K. Venkatraman, N. Vijayakumar, V. Kanimozhi, S. M. Arbaaz, R. G. S. Stacey, J. Anusha, R. Choudhary, V. Lvov, G. I. Tovar, F. Senatov, S. Koppala and S. Swamiappan, *J. Hazard. Mater. Adv.*, 2022, **7**, 100094.
10 A. E. Charkiewicz, W. J. Omeljaniuk, K. Nowak, M. Garley and J. Nikliński, *Molecules*, 2023, **28**, 1–16.
11 D. M. Templeton, *Anal. Bioanal. Chem.*, 2003, **375**, 1062–1066.
12 J. P. Barnett, D. J. Scanlan and C. A. Blindauer, *Anal. Bioanal. Chem.*, 2012, **402**, 3311–3322.
13 S. A. Manley and J. Gailer, *Expert Rev. Proteomics*, 2009, **6**, 251–265.
14 M. A. Da Silva, A. Sussulini and M. A. Arruda, *Expert Rev. Proteomics*, 2010, **7**, 387–400.
15 A. Lothian, D. J. Hare, R. Grimm, T. M. Ryan, C. L. Masters and B. R. Roberts, *Front. Aging Neurosci.*, 2013, **5**, 1–7.
16 J. P. C. Coverdale, S. Polepalli, M. A. Z. Arruda, A. B. S. da Silva, A. J. Stewart and C. A. Blindauer, *Biomolecules*, 2024, **14**, 104.
17 J. L. Gómez-Ariza, E. Z. Jahromi, M. González-Fernández, T. García-Barrera and J. Gailer, *Metallomics*, 2011, **3**, 566–577.
18 N. Jakubowski, R. Lobinski and L. Moens, *J. Anal. At. Spectrom.*, 2004, **19**, 1–4.
19 D. Pröfrock and A. Prange, *Appl. Spectrosc.*, 2012, **66**, 843–868.
20 A. Sussulini and J. S. Becker, *Metallomics*, 2011, **3**, 1271–1279.
21 A. B. Nowakowski, W. J. Wobig and D. H. Petering, *Metallomics*, 2014, **6**, 1068–1078.
22 O. O. Ajayi, *J. Prog. Eng. Phys. Sci.*, 2024, **3**, 23–31.
23 Y. Lin and M. L. Gross, *Biomolecules*, 2022, **12**, 135.
24 Y. Y. Chang, H. Li and H. Sun, *Inorg. Organomet. Transition Met. Complexes Biol. Mol. Living Cells*, 2017, 329–353.
25 J. Ward, E. Ollmann, E. Maxey and L. A. Finney, *Methods Mol. Biol.*, 2014, **1876**, 171–187.
26 I. I. Fedorov, V. I. Lineva, I. A. Tarasova and M. V. Gorshkov, *Biochemistry*, 2022, **87**, 983–994.
27 N. Ye, F. Zhou, X. Liang, H. Chai, J. Fan, B. Li and J. Zhang, *Biomed Res. Int.*, 2022, **1**, 8965712.
28 S. A. Manley, S. Byrns, A. W. Lyon, P. Brown and J. Gailer, *J. Biol. Inorg. Chem.*, 2009, **14**, 61–74.
29 J. Szpunar, *Analyst*, 2005, **130**, 442.
30 S. Mounicou, J. Szpunar and R. Lobinski, *Eur. J. Mass Spectrom.*, 2010, **16**, 243–253.
31 Y. Tang, L. Liu, Q. Zhou, D. Wang, H. Guo, N. Liu, X. Yan, Z. Wang, B. He, L. Hu and G. Jiang, *J. Chromatogr. B: Anal. Technol. Biomed. Life Sci.*, 2024, **1243**, 124235.
32 S. El Balkhi, J. Poupon, J. M. Trocello, F. Massicot, F. Woimant and O. Laprévote, *Anal. Chem.*, 2010, **82**, 6904–6910.
33 R. González-Domínguez, Size Fractionation of Metal Species from Serum Samples for Studying Element Biodistribution in Alzheimer's Disease, *Metals in the brain : measurement and imaging*, ed. A. R. White, Springer New York, New York, NY, 2017, vol. 124, pp. 127–149.
34 B. Michalke, A. Berthele, P. Mistriotis, M. Ochsenkühn-Petropoulou and S. Halbach, *J. Trace Elem. Med. Biol.*, 2007, **21**, 4–9.
35 P. Jitaru, H. Goenaga-Infante, S. Vaslin-Reimann and P. Fisicaro, *Anal. Chim. Acta*, 2010, **657**, 100–107.
36 V. Lopez-Avila, O. Sharpe and W. H. Robinson, *Anal. Bioanal. Chem.*, 2006, **386**, 180–187.
37 B. Michalke, S. Halbach, A. Berthele, P. Mistritiotis and M. Ochsenkühn-Petropoulou, *J. Anal. At. Spectrom.*, 2007, **22**, 267–272.
38 P. Moreno, M. A. Quijano, A. M. Gutiérrez, M. C. Pérez-Conde and C. Cámara, *Anal. Chim. Acta*, 2004, **524**, 315–327.
39 D. J. Hare, A. Grubman, T. M. Ryan, A. Lothian, J. R. Liddell, R. Grimm, T. Matsuda, P. A. Doble, R. A. Cherny, A. I. Bush, A. R. White, C. L. Masters and B. R. Roberts, *Metallomics*, 2013, **5**, 1656–1662.
40 L. Peng, M. He, B. Chen, Y. Qiao and B. Hu, *ACS Nano*, 2015, **9**, 10324–10334.
41 H. Haraguchi, in *Metallomics*, Springer Japan, Tokyo, 2017, vol. 19, pp. 3–39.
42 M. Malavolta, F. Piacenza, A. Basso, R. Giacconi, L. Costarelli, S. Pierpaoli and E. Mocchegiani, *Anal. Biochem.*, 2012, **421**, 16–25.
43 P. Heitland and H. D. Köster, *J. Trace Elem. Med. Biol.*, 2021, **64**, 126706.

44 N. Laur, R. Kinscherf, K. Pomytkin, L. Kaiser, O. Knes and H.-P. Deigner, *PLoS One*, 2020, **15**, e0233357.
45 L. A. Currie, *Pure Appl. Chem.*, 1995, **67**, 1699–1723.
46 V. J. Barwick, S. L. R. Ellison and B. Fairman, *Anal. Chim. Acta*, 1999, **394**, 281–291.
47 S. Hann, G. Koellensperger, C. Obinger, P. G. Furtmüller and G. Stingeder, *J. Anal. At. Spectrom.*, 2004, **19**, 74–79.
48 M. F. Mesko, C. A. Hartwig, C. A. Bizzi, J. S. F. Pereira, P. A. Mello and E. M. M. Flores, *Int. J. Mass Spectrom.*, 2011, **307**, 123–136.
49 I. F. Seregina, K. Osipov, M. A. Bol'shov, D. G. Filatova and S. Y. Lanskaya, *J. Anal. Chem.*, 2019, **74**, 182–191.
50 B. L. Batista, J. L. Rodrigues, J. A. Nunes, V. C. de Oliveira Souza and F. Barbosa, *Anal. Chim. Acta*, 2009, **639**, 13–18.
51 E. Pruszkowski and K. Neubauer, *PerkinElmer Application Note*, 2017.
52 Z. S. Gong, X. H. Jiang, C. Q. Sun, Y. P. Tian, G. H. Guo, Y. Z. Zhang, X. H. Zhao and Y. Wang, *Int. J. Mass Spectrom.*, 2017, **423**, 20–26.
53 B. D. Kerger, R. Gerads, H. Gurleyuk, K. A. Thuett, B. L. Finley and D. J. Paustenbach, *Toxicol. Environ. Chem.*, 2013, **95**, 687–708.
54 M. Sokołowska, M. Wszelaka-Rylik, J. Poznański and W. Bal, *J. Inorg. Biochem.*, 2009, **103**, 1005–1013.
55 A. K. N. Nandedkar, M. S. Hong and F. Friedberg, *Biochem. Med.*, 1974, **9**, 177–183.
56 U. H. Stenman, K. Simons and R. Gräsbeck, *Scand. J. Clin. Lab. Invest.*, 1968, **21**, 202–210.
57 S. Al-Harthi, J. I. Lachowicz, M. E. Nowakowski, M. Jaremko and Ł. Jaremko, *J. Inorg. Biochem.*, 2019, **198**, 110716.
58 M. Odaka, M. Kobayashi and L. Science, *Encycl. Met.*, 2013, pp. 670–678.
59 J.-L. Guéant and F. Namour, in *Encyclopedia of Gastroenterology*, Elsevier, 2004, vol. 12, pp. 619–624.
60 N. E. L. Saris, E. Mervaala, H. Karppanen, J. A. Khawaja and A. Lewenstam, *Clin. Chim. Acta*, 2000, **294**, 1–26.
61 M. H. Kroll and R. J. Elin, *Clin. Chem.*, 1985, **31**, 244–246.
62 R. Swaminathan, *Clin. Biochem. Rev.*, 2003, **24**, 47–66.
63 D. A. Goldstein, in *Clinical Methods: The History, Physical, and Laboratory Examinations*, ed. H. K. Walker, W. D. Hall and J. W. Hurst, Boston, 3rd edn, 1990, vol. 313, p. 1248.
64 G. Merlini, L. A. Fitzpatrick, E. S. Siris, J. P. Bilezikian, S. Birken, S. Beychok and E. F. Osserman, *J. Clin. Immunol.*, 1984, **4**, 185–196.
65 N. Liu, L. S. Lo, S. H. Askary, L. Jones, T. Z. Kidane, T. T. M. Nguyen, J. Goforth, Y.-H. Chu, E. Vivas, M. Tsai, T. Westbrook and M. C. Linder, *J. Nutr. Biochem.*, 2007, **18**, 597–608.
66 S. L. Marklund, *J. Clin. Invest.*, 1984, **74**, 1398–1403.
67 I. Zaitseva, V. Zaitsev, G. Card, K. Moshkov, B. Bax, A. Ralph and P. Lindley, *J. Biol. Inorg. Chem.*, 1996, **1**, 15–23.
68 P. L. Wirth and M. C. Linder, *JNCI, J. Natl. Cancer Inst.*, 1985, **75**, 277–284.
69 S. L. Marklund, E. Holme and L. Hellner, *Clin. Chim. Acta*, 1982, **126**, 41–51.
70 P. Z. Neumann and A. Sass-Kortsak, *J. Clin. Invest.*, 1967, **46**, 646–658.
71 T. Kirsipuu, A. Zadorožnaja, J. Smirnova, M. Friedemann, T. Plitz, V. Tõugu and P. Palumaa, *Sci. Rep.*, 2020, **10**, 1–11.
72 K. Marković, M. Cemazar, G. Sersa, R. Milačič and J. Ščančar, *J. Anal. At. Spectrom.*, 2022, **37**, 1675–1686.
73 N. F. Adham, M. K. Song and H. Rinderknecht, *Biochim. Biophys. Acta, Protein Struct. Mol. Enzymol.*, 1977, **495**, 212–219.
74 W. Bal, M. Sokołowska, E. Kurowska and P. Faller, *Biochim. Biophys. Acta, Gen. Subj.*, 2013, **1830**, 5444–5455.
75 E. L. Giroux, *Biochem. Med.*, 1975, **266**, 258–266.
76 J. P. C. Coverdale, J. P. Barnett, A. H. Adamu, E. J. Griffiths, A. J. Stewart and C. A. Blindauer, *Metallomics*, 2019, **11**, 1805–1819.
77 B. Chen, P. Yu, W. N. Chan, F. Xie, Y. Zhang, L. Liang, K. T. Leung, K. W. Lo, J. Yu, G. M. K. Tse, W. Kang and K. F. To, *Signal Transduction Targeted Ther.*, 2024, **9**, 6.
78 J. W. Foote and H. T. Delves, *J. Clin. Pathol.*, 1984, **37**, 1050–1054.
79 S. Fernández-Menéndez, M. L. Fernández-Sánchez, B. Fernández-Colomer, R. R. de la Flor, St. Remy, G. D. C. Cotallo, A. S. Freire, B. F. Braz, R. E. Santelli and A. Sanz-Medel, *J. Chromatogr. A*, 2016, **1428**, 246–254.
80 R. R. Alves Peixoto, S. Fernández-Menéndez, B. Fernández-Colomer, A. I. Pérez Vaquero, S. Cadore, A. Sanz-Medel and M. L. Fernández-Sánchez, *J. Food Compos. Anal.*, 2020, **87**, 103395.
81 A. M. N. Silva, T. Moniz, B. de Castro and M. Rangel, *Coord. Chem. Rev.*, 2021, **449**, 214186.
82 A. M. N. Silva and M. Rangel, *Molecules*, 2022, **27**, 1784.
83 W. Wang, M. A. Knovich, L. G. Coffman, F. M. Torti and S. V. Torti, *Biochim. Biophys. Acta, Gen. Subj.*, 2010, **1800**, 760–769.
84 M. Aschner, K. E. Vrana and W. Zheng, *Neurotoxicology*, 1999, **20**, 173–180.
85 L. Davidsson, B. Lönnerdal, B. Sandström, C. Kunz and C. L. Keen, *J. Nutr.*, 1989, **119**, 1461–1464.
86 O. Rabin, L. Hegedus, J. Bourre and Q. R. Smith, *J. Neurochem.*, 1993, **61**, 509–517.
87 J. Crossgrave and W. Zheng, *NMR Biomed.*, 2004, **17**, 544–553.
88 B. Michalke, S. Halbach, A. Berthele, P. Mistritiotis and M. Ochsenkühn-Petropoulou, *J. Anal. At. Spectrom.*, 2007, **22**, 267–272.
89 K. Neth, M. Lucio, A. Walker, B. Kanawati, J. Zorn, P. Schmitt-Kopplin and B. Michalke, *Chem. Res. Toxicol.*, 2015, **28**, 1434–1442.
90 M. Peana, E. Gumienna-Kontecka, F. Piras, M. Ostrowska, K. Piasta, K. Krzywoszynska, S. Medici and M. A. Zoroddu, *Inorg. Chem.*, 2020, **59**, 4661–4684.
91 D. Ç. Demir, H. Demir, N. Bozan, Ş. Belli and C. Demir, *J. Elementol.*, 2023, **28**, 89–106.
92 H. Li, X. Li, J. Liu, L. Jin, F. Yang, J. Wang and O. Wang, *Int. J. Environ. Health Res.*, 2017, **3123**, 1–11.
93 A. J. A. Al-Modhefer, M. W. B. Bradbury and T. J. B. Simons, *Clin. Sci.*, 1991, **81**, 823–829.
94 Q. Nong, B. Chen, Y. Huang, Y. Li, Y. Wang, L. Liu, B. He, T. Luan, L. Hu and G. Jiang, *Chemosphere*, 2023, **341**, 140138.

95 V. Mostert, *Arch. Biochem. Biophys.*, 2000, **376**, 433–438.
96 K. R. Maddipati and L. J. Marnett, *J. Biol. Chem.*, 1987, **262**, 17398–17403.
97 I. Harrison, D. Littlejohn and G. S. Fell, *Analyst*, 1996, **121**, 189–194.
98 S. Letsiou, Y. Lu, T. Nomikos, S. Antonopoulou, D. Panagiotakos, C. Pitsavos, C. Stefanadis and S. A. Pergantis, *Proteomics*, 2010, **10**, 3447–3457.
99 M. E. Wastney, G. F. Combs, W. K. Canfield, P. R. Taylor, K. Y. Patterson, A. D. Hill, J. E. Moler and B. H. Patterson, *J. Nutr.*, 2011, **141**, 708–717.
100 Y. Gao, Y. Liu, G. Deng and Z. Wang, *Biol. Trace Elem. Res.*, 2004, **100**, 105–115.
101 Ò. Palacios, J. Ruiz Encinar, D. Schaumlöffel and R. Lobinski, *Anal. Bioanal. Chem.*, 2006, **384**, 1276–1283.
102 Y. Suzuki, T. Sakai and N. Furuta, *Anal. Sci.*, 2012, **28**, 221–224.
103 V. Mostert, I. Lombeck and J. Abel, *Arch. Biochem. Biophys.*, 1998, **357**, 326–330.
104 C. Méplan, F. Nicol, B. T. Burtle, L. K. Crosley, J. R. Arthur, J. C. Mathers and J. E. Hesketh, *Antioxid. Redox Signaling*, 2009, **11**, 2631–2640.
105 S. A. Rupa, M. A. M. Patwary, M. M. Matin, W. E. Ghann, J. Uddin and M. Kazi, *Toxicol. Res.*, 2023, **12**, 355–368.
106 Y. Li, B. He, Q. Nong, G. Qu, L. Liu, J. Shi, L. Hu and G. Jiang, *Chem. Commun.*, 2018, **54**, 7439–7442.
107 C. Chen, H. Yu, J. Zhao, B. Li, L. Qu, S. Liu, P. Zhang and Z. Chai, *Environ. Health Perspect.*, 2006, **114**, 297–301.
108 Z. Yun, L. Li, L. Liu, B. He, X. Zhao and G. Jiang, *Metallomics*, 2013, **5**, 821–827.
109 G. Morrison, *Clin. Methods Hist. Phys. Lab. Exam.*, 1990, pp. 890–894.
110 T. W. May, R. H. Wiedmeyer, U. S. G. Survey and B. R. Division, *At. Spectrosc.*, 1998, **19**, 150–155.